Mechanocatalytic Hydrogenolysis of a Benzyl Phenyl Ether over Supported Nickel Catalysts

Supplementary Information

Andrew W. Tricker[a,b], Sean Najmi[a], Erin V. Phillips[a,b], Karoline L. Hebisch[a], Jason X. Kang[a],
Carsten Sievers[a,b,]*

[a]*School of Chemical & Biomolecular Engineering, Georgia Institute of Technology, Atlanta, GA 30332*
[b]*Renewable Bioproducts Institute, Georgia Institute of Technology, Atlanta, GA 30332*

*Corresponding Author:

Carsten Sievers
Phone: +1 (404) 385-7685
Email: carsten.sievers@chbe.gatech.edu

The number of pages: 13

The number of figures: 10

The number of tables: 2

S1 Characterization of Fresh Catalyst

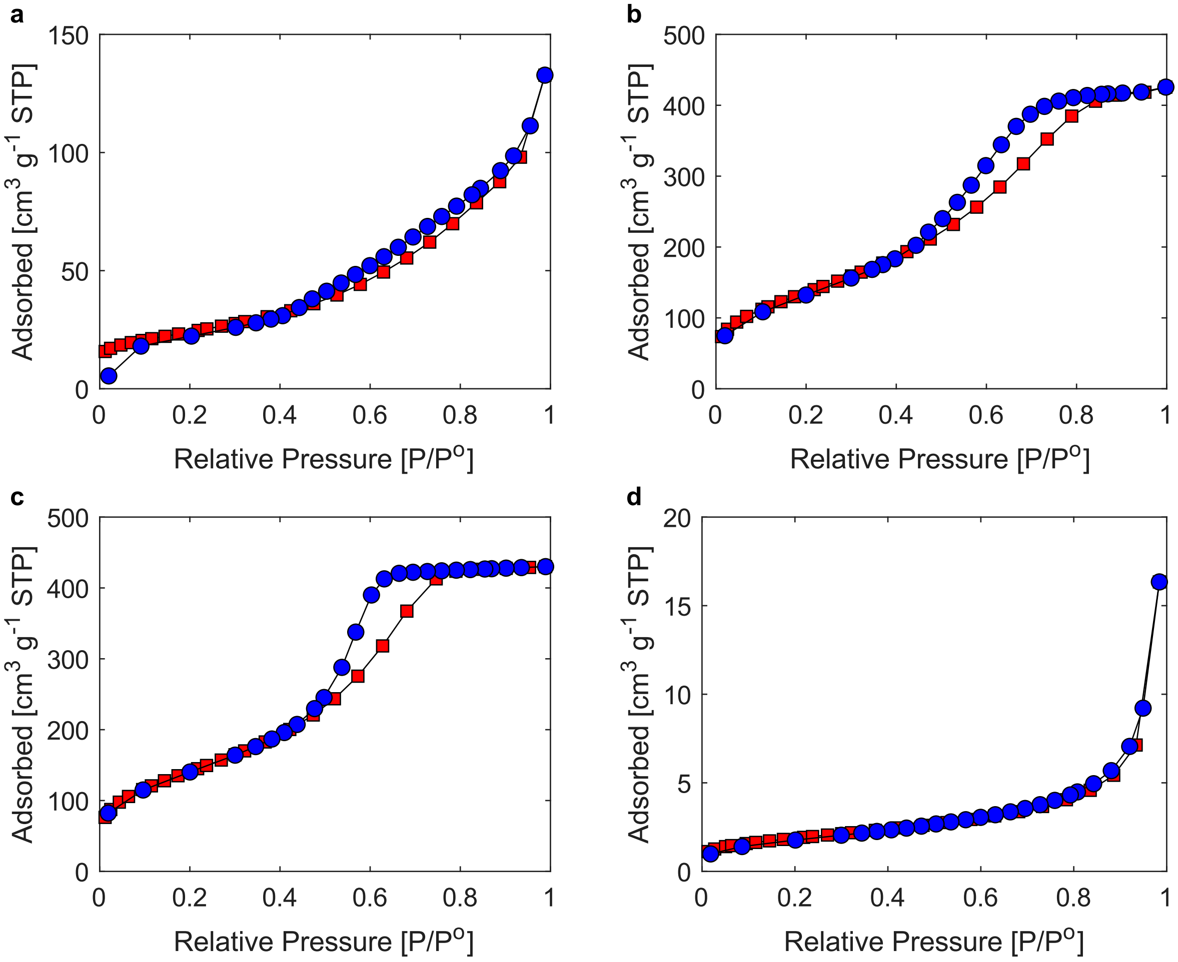

Fig. S1: N_2 physisorption adsorption (red) and desorption (blue) isotherms for (a) $Ni_{53}SiAl$, (b) $Ni_{05}SiAl$, (c) $Ni_{05}Si_{High}$, and (d) $Ni_{05}Si_{Low}$.

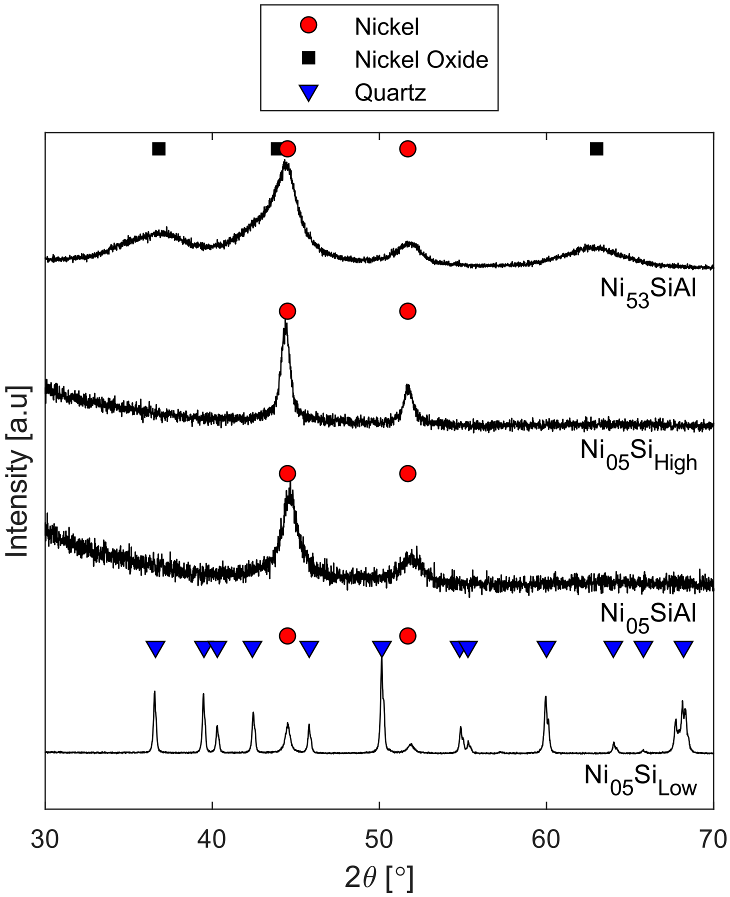

Fig. S2: X-ray diffractograms of the fresh catalysts with peak assignment.

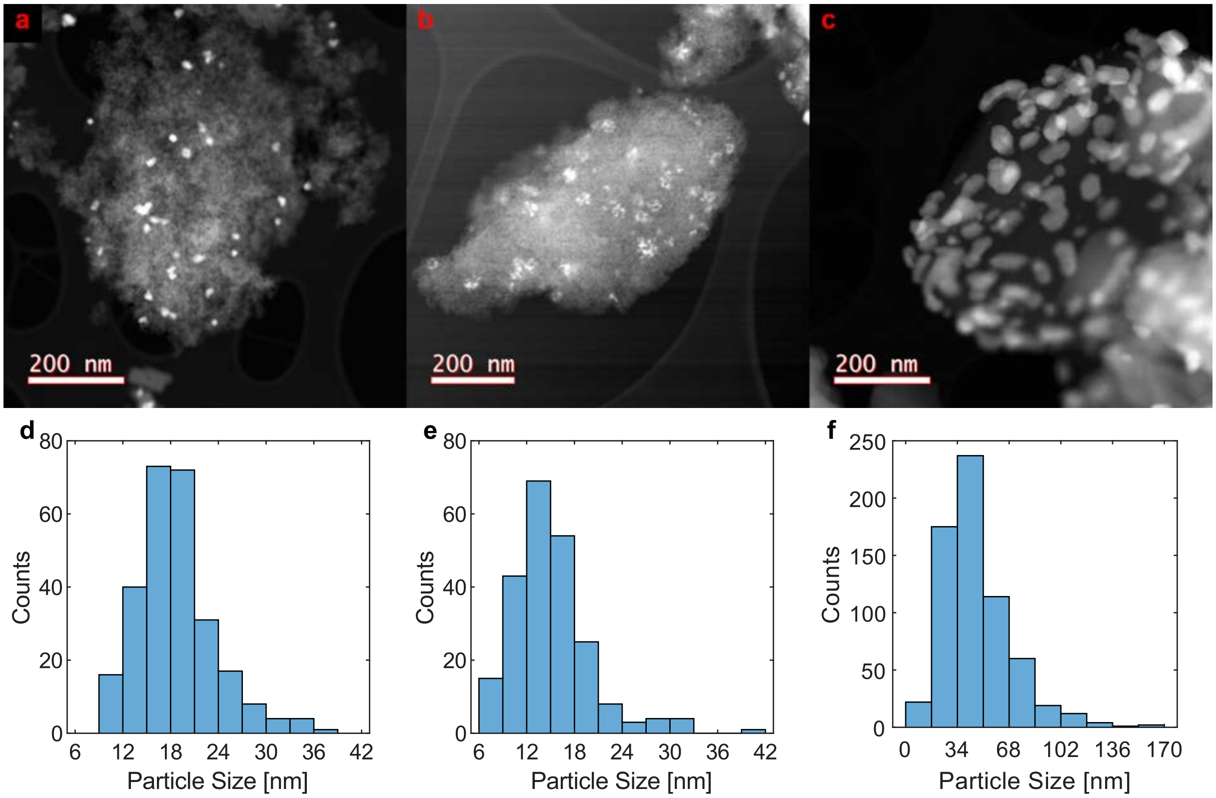

Fig. S3: Example STEM images of (a) $Ni_{05}SiAl$, (b) $Ni_{05}Si_{High}$, and (c) $Ni_{05}Si_{Low}$ for particle size analysis and histograms of all measured particles for (d) $Ni_{05}SiAl$, (e) $Ni_{05}Si_{High}$, and (f) $Ni_{05}Si_{Low}$.

S2 Mechanocatalytic Hydrogenolysis Reaction Results

S2.1 Hydrogenolysis using H_2

Table S1: Complete Raw Data Results of the Hydrogenolysis Reactions

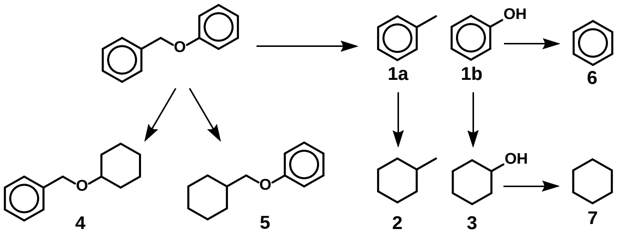

Entry	Catalyst	Milling Time [min]	BPE Conv. [%]	Yields [%]								Carbon Balance [%]
				1a	1b	2	3	4	5	6	7	
1	$Ni_{53}SiAl$	7.5	15.7	6.94	6.57	0	0	0	0.02	0	0	91.2
2	$Ni_{53}SiAl$	30	47.9	38.0	25.4	0.05	2.38	0.14	0.32	0	0	85.8
3	$Ni_{53}SiAl$	60	77.5	64.1	32.4	0.16	11.8	0.43	0.96	0.09	0	78.9
4	$Ni_{53}SiAl$ (Cycle 1)	120	99.6	88.2	30.4	0.13	28.34	0.36	0.89	0.22	0.08	76.5
5	$Ni_{53}SiAl$	180	99.9	89.6	17.3	0.12	42.1	0.11	0.57	0.26	0.18	76.7
6	$Ni_{53}SiAl$ (Cycle 2)	240	99.0	66.6	19.5	1.56	43.5	0.51	2.13	0.32	0.20	69.6
7	$Ni_{53}SiAl$ (Cycle 3)	240	65.1	28.1	12.2	0.42	10.8	1.19	3.15	0.36	0.18	65.4
8	$Ni_{05}SiAl$	180	76.5	5.77	5.89	0.08	0.62	0.10	0.63	0.44	0.37	23.5
9	$Ni_{05}Si_{High}$	180	82.2	8.96	8.35	0.05	1.46	0.06	0.43	0.41	0.17	28.0
10	$Ni_{05}Si_{Low}$	180	29.0	13.9	5.16	0.28	0.48	0.20	1.44	0.84	0.55	83.5

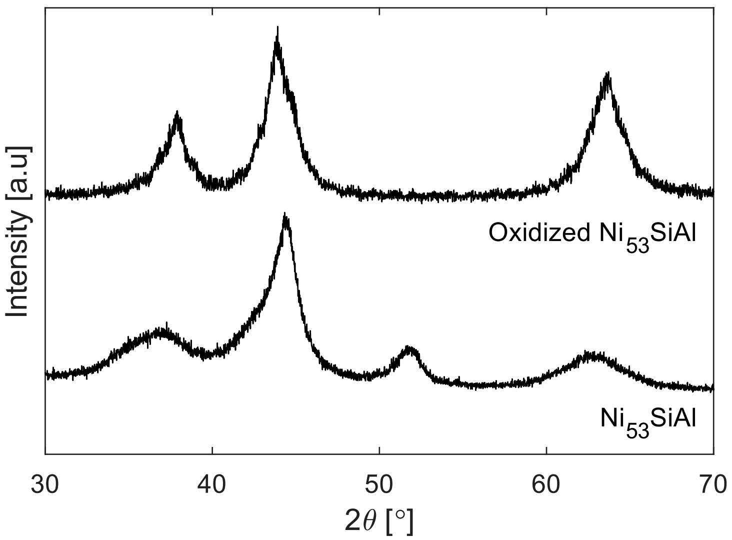

Fig. S4: X-ray diffractogram of fresh $Ni_{53}SiAl$ (bottom) and of oxidized $Ni_{53}SiAl$ (top).

S2.2 Hydrogenolysis via a Hydrogen Transfer Agent

To test the feasibility of isopropanol as a hydrogen transfer agent, three experiments were performed, in which BPE was milled with the $Ni_{53}SiAl$ catalyst in the presence of IPA and without H_2. Initially, the ball mill set up was modified to include a bubbler filled with IPA before the milling vessel. Here, IPA saturated N_2 (15 sccm) was fed during the extent of milling, but no products were detected after 180 min. Next, IPA (125 μL) was added directly to the vessel at the beginning of the experiment to ensure sufficient IPA was present. Here, the vessel was closed off and the milling did not occur in a flowing atmosphere. Again, after milling for 180 min, no products were detected. Finally, IPA was again added to the milling vessel (125 μL), but the reaction was conducted in a continuous flow of N_2. Here, a 2.4% yield of toluene and a 1.6% yield of phenol was measured after 180 min. In principle, IPA can work as a hydrogen transfer agent for mechanocatalytic hydrogenolysis.

S3 Ni_{53}SiAl Recycling Reactions and Spent Catalyst Characterization

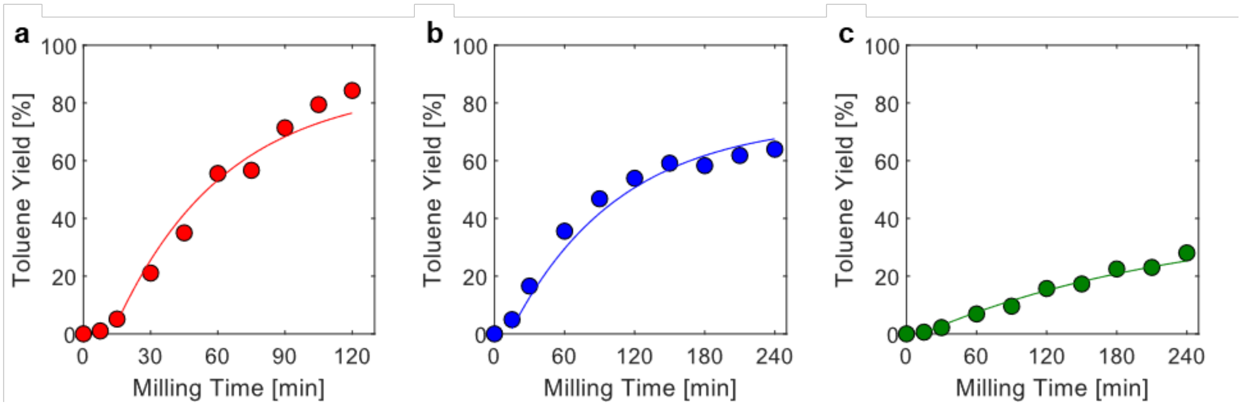

Fig. S5: Independent kinetic fits for (a) Cycle 1, (b) Cycle 2, and (c) Cycle 3 with Ni_{53}SiAl. 1.00 g Ni_{53}SiAl, 0.20 g BPE, 25 mL S.S. vessel, 2x15 mm S.S. grinding balls, 30 Hz, 60 sccm H_2.

Table S2: Relative peak areas of the G, D_1, and D_2 Raman band of Spent Ni_{53}SiAl.

Raman Band [cm^{-1}]	2 h	6 h	10 h
G [1350]	45.56	44.99	48.13
D_1 [1580]	48.83	47.23	42.36
D_2 [1620]	5.61	7.79	9.51

Agglomeration, attrition, and oxidation of the nickel were also explored as potential sources of deactivation. EDS mapping of the spent catalyst did not show separation of the nickel from the support or agglomeration the nickel particles on the support (Figure S6). Additionally, agglomeration of the nickel particles is not expected to have a significant impact on the observed rate of hydrogenolysis. Significant agglomeration was observed for the spent Ni_{05}SiAl and $Ni_{05}Si_{Low}$ but not for $Ni_{05}Si_{High}$, while the hydrogenolysis rates were similar between the three catalysts (*vide infra*). Since the nickel is located on the exterior of the support, attrition could lead to a loss of nickel particles during milling. However, elemental analysis showed no significant change in the Ni:Al ratio between the fresh and spent catalysts (Figure S7). Finally, since the catalyst was exposed to air between cycles, the newly exposed metallic surfaces are expected to oxidize. XRD of the spent catalysts (Figure S8) showed negligible amounts of bulk oxidation, so the new passivating oxide layers are expected to be thin and removed during milling similar to the fresh catalyst. Consequently, to our current understanding, the formation of carbon deposits is the most reasonable explanation for the deactivation of the catalyst, but future work will be necessary to elucidate the exact mechanism of the deactivation and to identify prevention strategies.

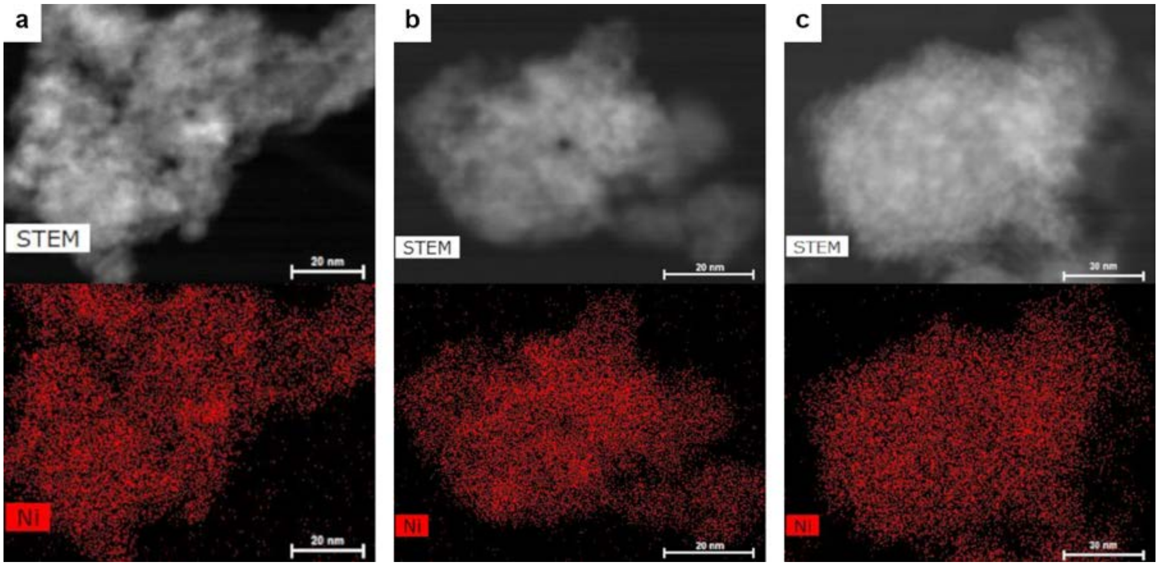

Fig. S6: STEM and EDS mapping of $Ni_{53}SiAl$ after (a) Cycle 1, (b) Cycle 2, and (c) Cycle 3.

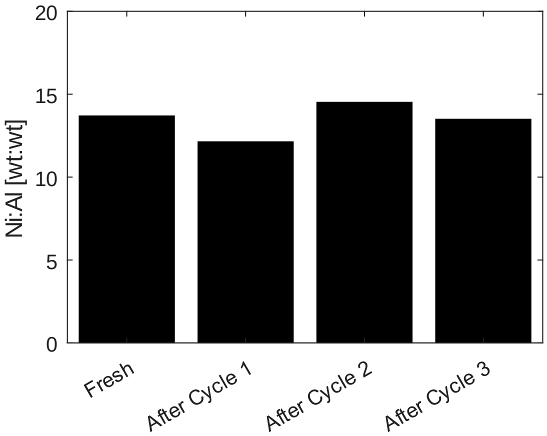

Fig. S7: Ni:Al Ratio of spent $Ni_{53}SiAl$ as determined by ICP-OES.

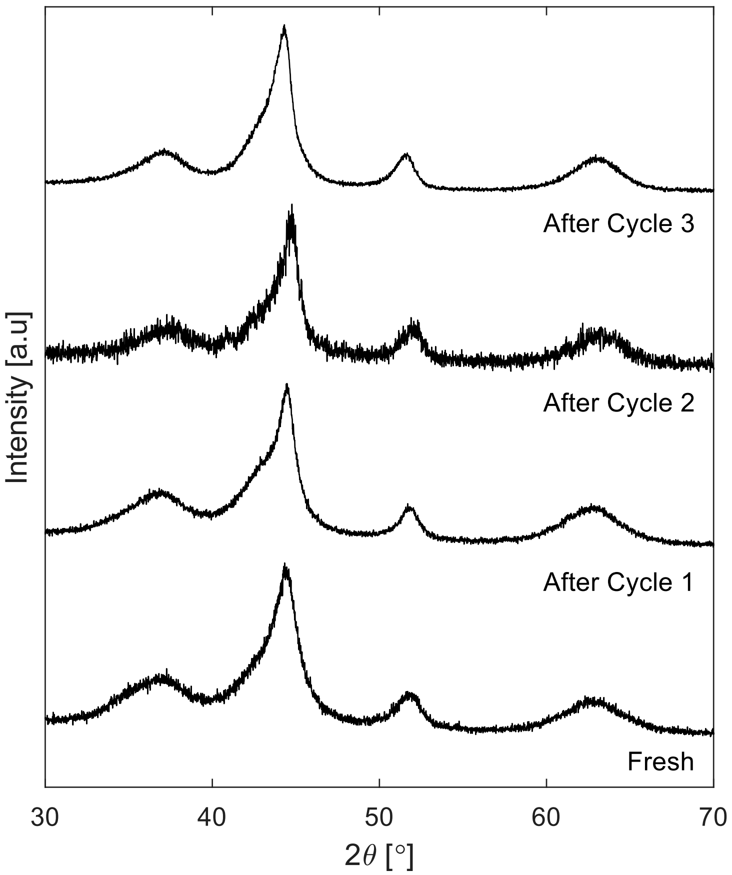

Fig. S8: X-ray diffractograms of fresh and spent $Ni_{53}SiAl$ samples.

S4 Hydrodeoxygenation of Guaiacol

Guaiacol (0.2 g) was milled with the $Ni_{53}SiAl$ catalyst (1.0 g) for 30 min, 60 min, and 180 min in H_2. In the initial experiments, after 30 min and 60 min, no products were detected and carbon balances were 44% and 40%, respectively. After 180 min, the products detected were catechol (0.11%), phenol (0.22%), and cyclohexanol (0.19%). Yields of these products were similar to the yields of HDO products during the hydrogenolysis of BPE (<1%). The carbon balance for this experiment increased to 62%, lower than but comparable to the carbon balance for the hydrogenolysis of BPE (77%).

S5 Characterization of Spent Low Nickel Catalysts

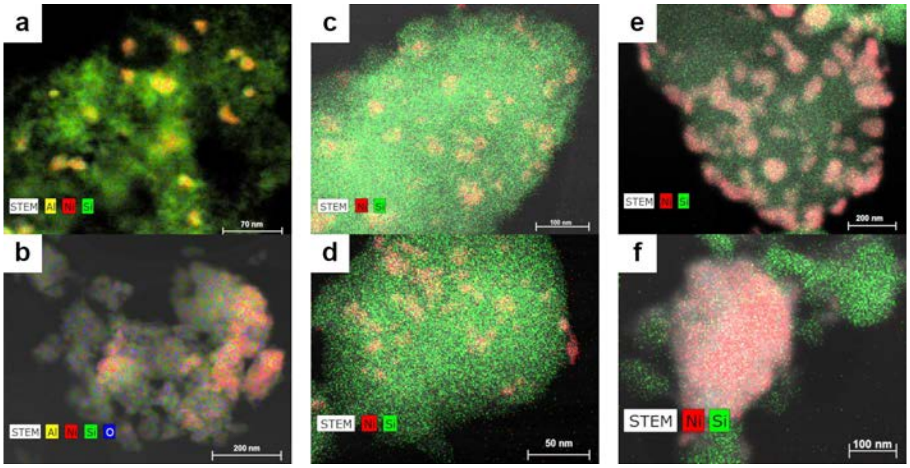

Fig. S9: EDS mapping of (a) fresh Ni$_{05}$SiAl and (b) spent Ni$_{05}$SiAl, (c) fresh Ni$_{05}$Si$_{High}$ and (d) spent Ni$_{05}$Si$_{High}$, and (e) fresh Ni$_{05}$Si$_{Low}$ and (f) spent Ni$_{05}$Si$_{Low}$. Yellow: Aluminum; Red: Nickel; Green: Silicon; Blue: Oxygen.

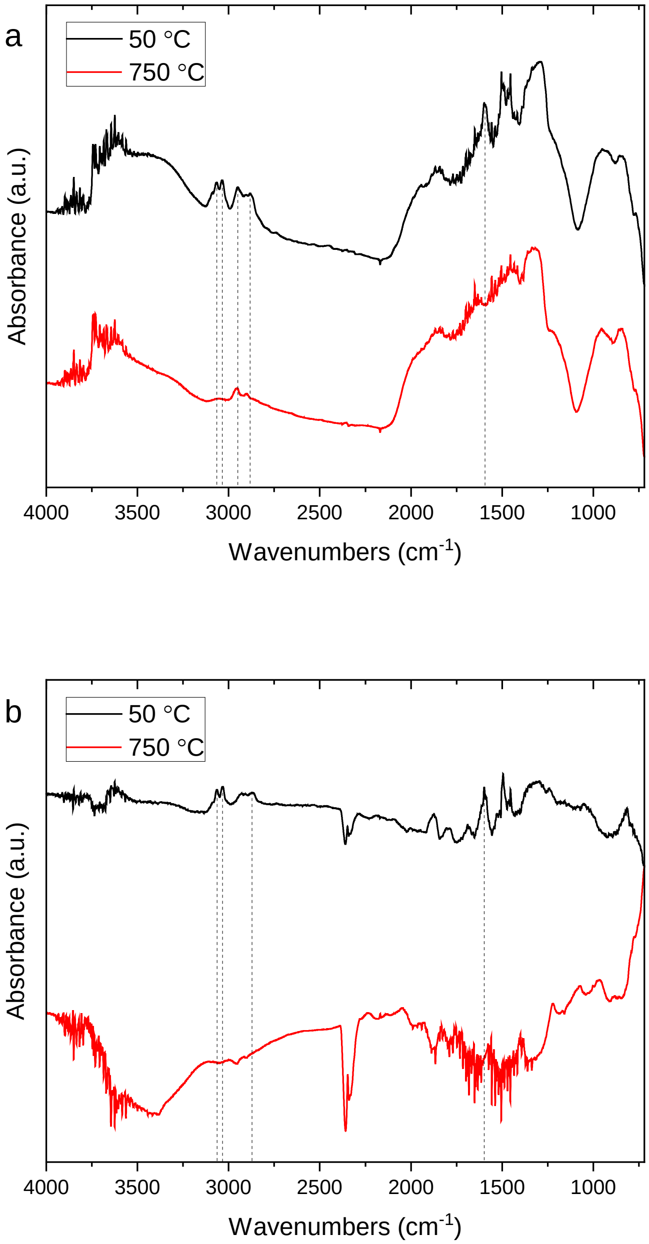

Fig. S10: (a) DRIFTS spectra of Ni$_{05}$Si$_{High}$ with pre-adsorbed BPE at 50 ºC (black) and after heating to 750 ºC (red) for 1 h in flow of 40 sccm N_2. (b) DRIFTS spectra of Ni$_{05}$Si$_{Low}$ with pre-adsorbed BPE at 50 ºC (black) and after heating to 750 ºC (red) for 1 h in flow of 40 sccm N_2.